Digital tanlock loop architecture with no delay

Omar Al-Kharji AL-Ali, Nader Anani, Saleh Al-Araji*,
Mahmoud Al-Qutayri* and Prasad Ponnapalli

School of Engineering, Manchester Metropolitan University, Manchester, UK
*College of Engineering, Khalifa University, Sharjah Campus, Sharjah, UAE.

Digital tanlock loop architecture with no delay

This paper proposes a new architecture for a digital tanlock loop which eliminates the time-delay block. The $\pi/2$ (rad) phase shift relationship between the two channels, which is generated by the delay block in the conventional time delay digital tanlock loop (TDTL), is preserved by using two quadrature sampling signals for the loop channels. The proposed system outperformed the original TDTL architecture, when both systems were tested with frequency shift keying (FSK) input signal. The new system demonstrated better linearity and acquisition speed as well as improved noise performance compared with the original TDTL architecture. Furthermore, the removal of the time-delay block enables all processing to be performed digitally which reduces the implementation complexity. Both the original TDTL and the new architecture without the delay block were modelled and simulated using MATLAB/Simulink. Implementation issues, including complexity and relation to simulation of both architectures are also addressed.

Keywords: time delay digital tanlock loop, no-delay digital tanlock loop, phase shifter, acquisition, locking range, jitters.

1. Introduction

Phase locked loops (PLLs) are widely used in communication systems for modulation, demodulation, and synchronization operations. For example, the receivers in modern wireless communication systems contain PLLs that perform carrier synchronization and symbol timing recovery tasks [1-3]. PLLs are also extensively used in microprocessors, digital signal processors and control systems [3-6].

The basic block diagram of a conventional PLL is shown in Figure 1. In this feedback system, the phase detector (PD) block compares the phase of the input "reference" signal (F_{ref}) with the phase of the output signal (F_N). The output of the PD is used to drive the voltage controlled oscillator (VCO) block. When the system is in its locked state, the negative feedback adjusts the VCO output so as to maintain a small and constant phase difference between the PD input signals. When this is achieved, the PD input signals will have the same frequency. The optional divider block ($\div$N) can be used to generate a low-noise high-frequency signal that is required in some applications [1,2,4].

Early generations of PLLs were designed using a variety of analogue circuit techniques. However, due to some inherent drawbacks of analogue circuits such as component tolerance and with the emergence of digital integrated circuit technologies, the design of an all digital PLL (DPLL) became a reality.
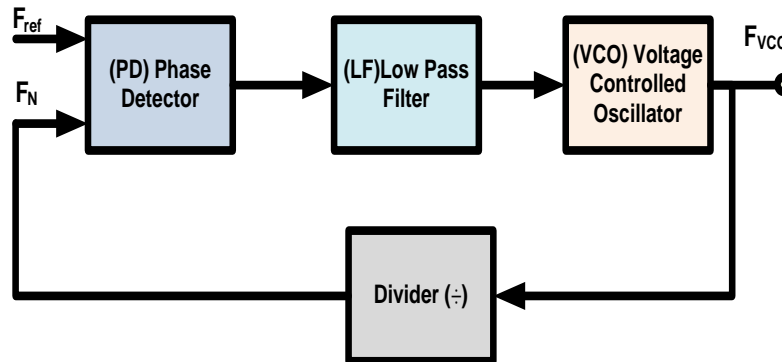

Figure 1. Block diagram of a typical analogue PLL.

The DPLL shown in Figure 2 is similar to the analogue PLL of Figure 1 except that the blocks are all digitally implemented. The digital phase detector (DPD) block is a phase-to-digital converter that senses the phase difference between input signal F_{ref} and the divided version (F_N) of the DCO (digital controlled oscillator) output signal (F_{DCO}). As stated earlier the divider block is optional. The output of the DPD is digitally filtered by the DLF (digital loop filter) and used to drive the DCO [7-9].
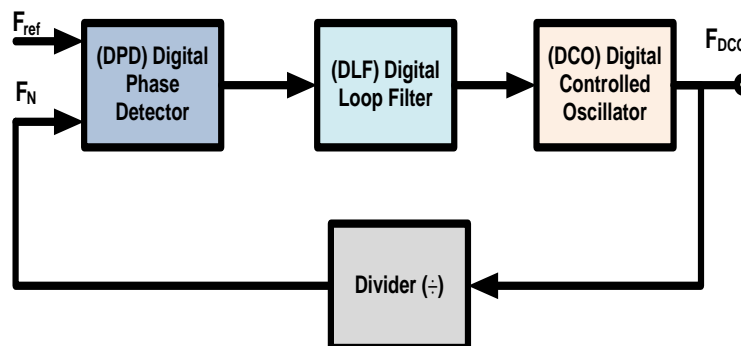

Figure 2. Block diagram of a typical digital PLL (DPLL).

The extensive literature on DPLLs has many architectures and implementation techniques for the block diagram of Figure 2. The various approaches depend upon the target application and the system implementation technology. A DPLL architecture that has a number of desirable attributes, which include linearity and insensitivity to variations in input signal power, is the time delay digital tanlock loop (TDTL) [10]. The TDTL solved the practical implementation issues that affected its predecessor, the digital tanlock loop (DTL), by replacing the Hilbert transformation (HT) block with a simple time delay unit [11]. Essentially, the TDTL consists of two sample and hold blocks, a phase detector, a digital filter, a digitally controlled oscillator, and a time-delay block. This mixed-signal system accepts an analogue signal at its input but performs all the processing digitally. This means that the system can be easily implemented in a digital or a mixed-signal process. However, the replacement of the HT by a time delay unit led to a slight degradation in the linearity of the locking range characteristic [12,13]. A number of possible solutions have been proposed in the literature to overcome this problem including the use of a variable time delay block [14-16]. This paper proposes an improved TDTL architecture that overcomes the nonlinearity problem through the elimination of the time delay block. This new no-delay DTL architecture is referred to as NDTL. The NDTL system modifies the design of the DCO circuitry so that two sampling signals with 90° phase shift are generated in order to maintain the quadrature relationship between the two channels of the system.

In this paper, section 2 presents the system architecture and analysis, while the noise analysis of the system is detailed in section 3. The testing results are presented in

section 4. The circuit implementation complexity of the system is discussed in section 5. Finally, the conclusions of the paper are given section 6.

2. NDTL System Architecture and Analysis

2.1 NDTL Architecture

The architecture of the proposed NDTL system is shown in Figure 3. The centre frequency of the DCO is set at twice the overall loop DCO (L-DCO) free-running frequency (f_0). The DCO signal is then used to drive the two counters whose outputs are used to sample the input signal x(t). Since there is a phase shift of 90° between the outputs of the counters, the quadrature relationship between the two sampling signals is preserved without the need for a phase-shifter in one of the channel's arms.
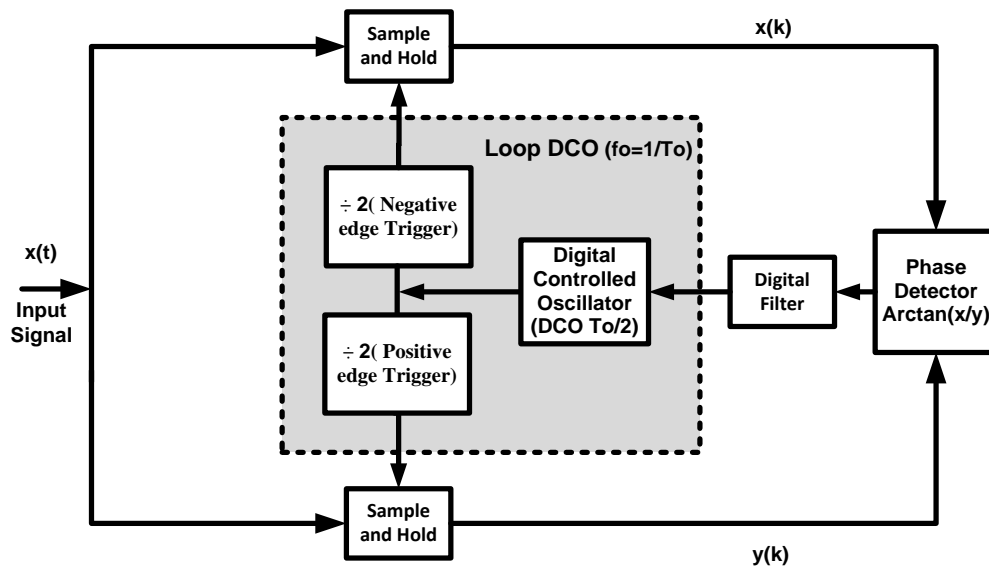

Figure 3. No delay digital tanlock Loop (NDTL).

2.2 NDTL analysis

Let the input signal to the loop be a sinusoid as given by Equation (1)

$$x(t) = A\sin[\omega_o t + \theta(t)] \tag{1}$$

where A is the amplitude of the signal, $\omega_o(\text{rad/s})$ is the free running frequency of the DCO, and $\theta(t)$ is the information bearing phase in radians. Following a similar analysis to that in [10,12,13], there are two sampling intervals of the DCO between the sampling instants $t(k+1)$ and $t(k)$ which are given by

$$T_1(k) = T_o - c(k-1) \tag{2}$$

$$T_2(k) = T_o - c(k-1) + \frac{\pi/2}{\omega_o} \tag{3}$$

where $T_o = 2\pi/\omega_o$ is the free-running period of the DCO, and $c(k-1)$ is the output of the digital filter at the previous sampling instant.

The total times up to the kth sampling instant for both sampling intervals can be defined as

$$t_1(k) = \sum_{i=1}^{k} T(i) = kT_o - \sum_{i=0}^{k-1} c(i) \tag{4}$$

and

$$t_2(k) = \sum_{i=1}^{k} T(i) = kT_o - \sum_{i=0}^{k-1} c(i) + \frac{\pi/2}{\omega_o} \tag{5}$$

The discretized signals generated by the samplers are

$$x(k) = Asin[\omega_o t_1 + \theta(k)] \tag{6}$$

$$y(k) = Asin[\omega_o t_2 + \theta(k)] \tag{7}$$

Substituting Equations (4) and (5) in Equations (6) and (7) respectively yields

$$x(k) = Asin\left[\theta(k) - \omega_o \sum_{i=0}^{k-1} c(i)\right] \tag{8}$$

$$y(k) = Asin\left[\theta(k) - \omega_o \sum_{i=0}^{k-1} c(i) \frac{\pi\omega_o}{2\omega}\right] = Acos\left[\theta(k) - \omega_o \sum_{i=0}^{k-1} c(i)\right] \tag{9}$$

The phase error between the input signal and the DCO is given by

$$\phi(k) = \theta(k) - \omega_o \sum_{i=0}^{k-1} c(i) \tag{10}$$

Therefore, both Equations (8) and (9) may be redefined as

$$x(k) = A\sin[\phi(k)] \tag{11}$$

$$y(k) = A\cos[\phi(k)] \tag{12}$$

When the signals $x(k)$ and $y(k)$ are applied to the phase detector, the generated error signal $e(k)$ between the two arms of the loop is

$$e(k) = f\left[\tan^{-1}\left(\frac{\sin\{\phi(k)\}}{\cos\{\phi(k)\}}\right)\right] = f[\tan^{-1}(\tan(\phi(k)))] = f[\phi(k)] \tag{13}$$

where $f(\gamma) = -\pi + (\gamma + \pi) \bmod 2\pi$ and $\phi(k)$ is the phase error.

Consequently, the degradation in the linearity of the TDTL system caused by the time-delay unit is eliminated [10,12,13].

Since $c(k) = D(z)e(k) = K_1' f[\phi(k)]$, where $D(z)$ is the loop filter transfer function and K_1' is the loop gain, two system difference equations can be derived from Equations (4), (5) and (13) as follows

$$\phi_1(k+1) = \phi(k) - \omega D(z)e(k) + \Lambda_o \tag{14}$$

$$\phi_2(k+1) = \phi(k) - \omega D(z)e(k) + \Lambda_o + \frac{\Lambda_o}{4} \tag{15}$$

From Equations (14) and (15) it can shown that

$$\phi_2(k+1) = \phi_1(k+1) + \frac{\Lambda_o}{4} = \phi_1(k+1) + \frac{\pi}{2}\left(\frac{\omega - \omega_o}{\omega_o}\right) \tag{16}$$

$$\phi_2(k+1) = \phi_1(k+1) + \frac{\pi}{2}\left(\frac{1-W}{W}\right) \tag{17}$$

Where $W = \omega_o/\omega$ and $\Lambda_o = 2\pi(\omega - \omega_o/\omega_o)$.

From Equation (17), it is evident that apart from a phase shift of $\pi/2$ (rad),

Equations (14) and (15) are similar. Therefore, the sampling signal given by Equation (2)

is used to follow the zero crossing of the incoming input signal whilst the shifted signal

of Equation (3) samples the input signal with a phase shift of 90°. This maintains the

quadrature relationship between the two channels without the need for a phase shifter for

the purpose of locking. Therefore the final difference equation is

$$\phi(k+1) = \phi(k) - \omega c(k) + \Lambda_o \tag{18}$$

2.2.1 *First order locking range analysis*

For the first order loop

$$c(k) = D(z)e(k) = K_1' f[\phi(k)] \tag{19}$$

Using Equations (1) and (3) and following a similar analysis to that in [10,12,13], the

difference equation and the locking range, depicted in Figure 4, for the NDTL first-order

system are given by Equations (20) and (21) respectively. The locking range of the first

order TDTL is also included in Figure 4 for comparison.

$$\phi(k+1) = \phi(k) - K_1'\phi(k) + \Lambda_o \tag{20}$$

$$2|1 - W| < K_1 < 2W \tag{21}$$

where $\phi(k)$ is the phase error at the instant k, $\Lambda_o = 2\pi(\omega - \omega_o)/\omega_o$, $K_1' = \omega G_1$, G_1

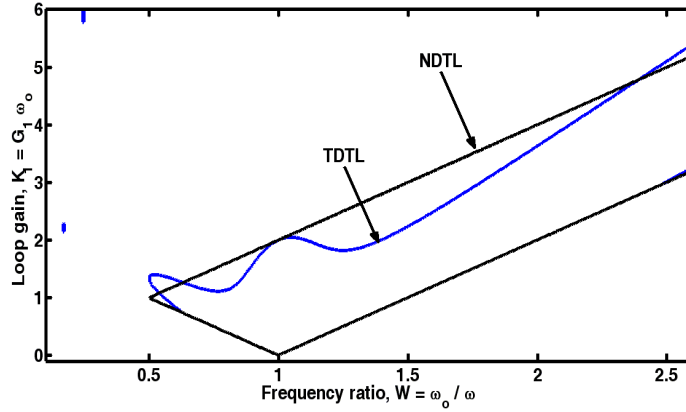is loop filter coefficient, $W = \omega_o/\omega$, and $K_1 = WK_1'$.

Figure 4. Locking range of both first order NDTL and TDTL.

2.2.2 Second order locking range analysis

Using Equations (1) and (3), for the second-order loop that uses the first-order accumulation digital filter with transfer function $D(z) = G_1 + G_2/(1 - z^{-1})$, the loop difference equation and the locking range, of Figure 5, are given by Equations (22) and Equations (23). Figure 5 shows also the locking range of the second order TDTL.

$$\phi(k + 2) = 2\phi(k + 1) - rK'_1 e(k + 1) + K'_1 e(k) - \phi(k) \tag{22}$$

$$0 < K_1 < \frac{4W}{1 + r} \ and \ r > 1 \tag{23}$$

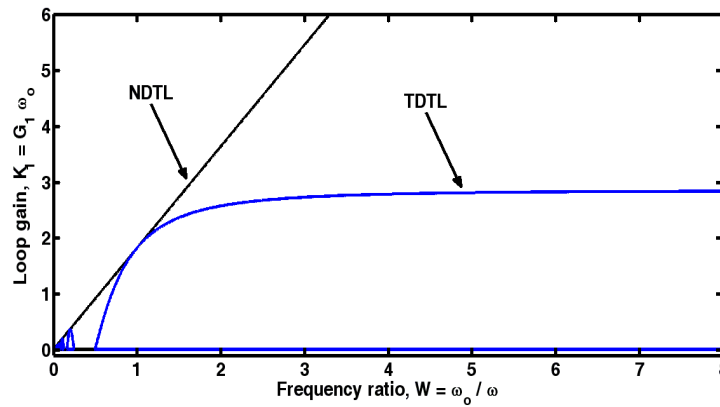where $r = 1 + G_1/G_2$, and G_1 and G_2 are the filter coefficients.

Figure 5. Locking range of both second order NDTL and TDTL.

3. Noise Analysis of the NDTL

The input signal is corrupted by an AWGN (additive white Gaussian noise) with a zero mean and two sided power spectrum density of $G_{nw}(f) = n_o/2$. Therefore, the autocorrelation can be given by the inverse Fourier Transform of $G_{nw}(f)$ as $R(\tau) = n_o\delta(\tau)/2$ [17,18], where $\delta(\tau)$ represents the Dirac Delta function. As a result, $R(\tau) = 0$ for $\tau \neq 0$ so any two different samples of this kind of noise are uncorrelated and for this reason they are statistically independent [19,20].

Since the NDTL has a discrete nature, the Chapman-Kolmogorov equation is used to study the statistical analysis of the phase error process [10-12]. The noise $\eta(k)$'s are mutually independent at any k instant. Therefore, the phase error process $\phi(k)$ can be regarded as a first order, discrete time, and continuously variable Markov process which is also governed by modulo 2π. The variable Markov process states that the first order Markov process depends only on the previous state. As a result with a given initial phase error $\phi(0)$, the probability density function (pdf) of $\phi(k)$ will satisfy the Chapman-Kolmogorov equation [10-12].

Assuming that the sampled noise process $\{\eta(k)\}$ is a sequence of independent and identical disturbances (iid) Gaussian random variables with zero mean and a variance σ_n^2, the noise samples $\{\eta'(k)\}$ (sampled the shifted signal of Equation (3)) is also an iid sequence with the same mean and variance.

Both inputs in Equations (11) and (12) are independent Gaussian random variables with the following statistical characteristics [11]

$$E[x(k)] = Asin\big(\phi(k)\big) \tag{24}$$

$$E[y(k)] = Acos\big(\phi(k)\big) \tag{25}$$

$$var[x] = var[y] = var[n] = var[n'] = \sigma_n^2 \tag{26}$$

Where n' is of the noise that is sampled at 90° phase shifts, $E[\ ]$ represents the expectation (mean) and $var[\ ]$ represents the variance. Consequently, the joint pdf $g(x, y)$ of the Gaussian random variables x and y is given by

$$g(x, y) = \frac{1}{2\pi\sigma_n^2} \exp\left[-\frac{1}{2\sigma_n^2}\{(x - Asin(\phi(k))^2 + (y - Acos(\phi(k))^2\}\right] \tag{27}$$

As AGWN has a disturbance effect on both amplitude and phase, both x and y can be redefined as in Equations (28) and (29) respectively.

$$x(k) = R_k sin(e(k)) \tag{28}$$

$$y(k) = R_k cos(e(k)) \tag{29}$$

where both random variables R_k and $e(k)$ have the following limits $0 < R_k < \infty$ and $-\pi < e(k) < \pi$. The joint pdf of both random variables R_k and $e(k)$ can be obtained from Equation (27) and the pdf $p[e(k)]$ can be computed by integrating over the range from zero to infinity with respect to R_k to get

$$p[e(k)] = \frac{1}{2\pi}\left[\exp(-\alpha)\right.$$
$$\left. + f(\alpha, k) \exp[-\alpha \, sin^2\{e(k) - \phi(k)\} \int_{-\infty}^{f(\alpha,k)} \exp(-\omega^2/2)] \, d\omega\right] \tag{30}$$

where $\alpha = A^2/2\sigma_n^2$ is the signal-to-noise ratio (SNR) and $f(\alpha, k) = \sqrt{2\alpha} \cos[e(k) - \phi(k)]$.

It is obvious that the peak of $p[e(k)]$ occurs at $e(k) = \phi(k)$ in the modulo 2π sense.

$e(k)$ is usually around $f[e(k)]$ in the presence of noise, and therefore can be decomposed into the term $f[e(k)]$ and the random variable $\eta(k)$ as in Equation (31).

$$e(k) = f[e(k)] + \eta(k) \tag{31}$$

where $\eta(k)$ lies in the interval $(-\pi - f[\phi(k)], \pi - f[\phi(k)])$.

Using Equations (30) and (31), the pdf of the random phase error noise disturbance p[η(k)]can be expressed from as

$$p(e) = \frac{1}{2\pi} \left[\exp(-\alpha) + \frac{\sqrt{\alpha}\cos\eta}{\sqrt{\pi}} \exp\{-\alpha \sin^2\eta\} \left\{ \frac{1}{2} + \mathrm{erf}\left[\sqrt{2\alpha}\, \cos\eta\right] \right\} \right] \tag{32}$$

where $\mathrm{erf}[x] = \frac{1}{\sqrt{2\pi}} \int_0^x \exp(-\omega^2/2)\, d\omega$

3.1 *Statistical behaviour of the first order NDTL in AGWN*

From Equation (20) the difference characteristic equation in the presence of noise of the first order NDTL can be expressed as

$$\phi(k+1) = \phi(k) - K_1' f[\phi(k)] + \Lambda_o + K_1' \eta(k) \tag{33}$$

The noise $\eta(k)$'s are mutually independent for different values of k. Therefore, the phase error process $\phi(k)$ can be regarded as a first order discrete time and continuously variable Markov process. The first order Markov process depends only on the previous state, so with a given initial phase error $\phi(0)$, the pdf of $\phi(k)$ will satisfy Chapman-Kolmogorov equation [10-12] in Equation (34).

$$p_{k+1}(\phi|\phi_o) = \int_{-\infty}^{\infty} q_k(\phi|u) p_k(u|\phi_o)\, du \tag{34}$$

where $p_{k+1}(\phi|\phi_o)$ is the pdf of $\phi(k)$ given an initial condition $\phi(0)$ and $q_k(\phi|u)$ is the transition pdf of $\phi(k+1)$ given $\phi(k)$.

If $\phi(k)$ is limited to $(-\pi, \pi)$, Equation (33) can be given by

$$\phi(k+1) = \phi(k) - K_1'\phi(k) + \Lambda_o + K_1'\eta(k) \tag{35}$$

By squaring both sides of Equation (35) and then taking the statistical expectation, the steady state variance can be attained as follows [11,19]

$$Var[\phi_{ss}] = \frac{K_1'}{2 - K_1'} E[\eta^2] = \int_{-\pi-E[\phi_{ss}]}^{\pi-E[\phi_{ss}]} \eta^2 \, p(\eta)\, d\eta \tag{36}$$

3.2   *Statistical behaviour of the second order NDTL in AGWN*

In the presence of noise and from Equation (22) the difference equation of the second-order NDTL is

$$\phi(k+1) = 2\phi(k+1) - rK_1'e(k+1) + K_1'e(k) - \phi(k) - rK_1'\eta(k+1) + K_1'\eta(k) \tag{37}$$

Equation (37) consists of two first-order difference equations that describe two Markov processes, which can be solved in a manner similar to the first-order DTL [11]. The mean and variance are given by Equations (38) and (39) respectively.

$$E[\phi_{ss}] = 0 \tag{38}$$

$$Var[\phi_{ss}] = \frac{2(r-1) + K_1'(r+1)}{4 - K_1'(r+1)} E[\eta^2] \tag{39}$$

4.   Simulation Results

The TDTL and the NDTL were modelled and subsequently simulated using MATLAB/Simulink. This enabled extensive performance evaluation of each architecture and subsequent comparison between them under the same input conditions. This section presents some of the extensive set of results used to compare NDTL and TDTL. The simulations were performed in both noisy and noise-free environments.

The performance of the first- and second-order NDTL systems was evaluated in comparison with that of the respective first- and second-order TDTL systems. The evaluation process included applying various sudden frequency steps and FSK input signals. The sudden frequency changes, which are either less or higher than the DCO free running frequency are indicated by a negative or a positive step respectively. This test is usually used to evaluate the acquisition time required by the system to reach its steady state [12].

Starting with frequency step test, in the noise free environment, Figure 6 illustrates the response to positive frequency steps for both the NDTL and the TDTL respectively. It can be seen that NDTL requires nearly one third of the time needed by the TDTL to achieve locking state. This is reflected in the much reduced number of samples that the NDTL requires to reach steady state. Another way to express the same results is to use phase plane plots which show the consecutive phase error samples $\phi(k)$ and $\phi(k+1)$ of both the NDTL and TDTL. The phase plane plots, following the application of a positive step, for the first- and second-order NDTL and TDTL are depicted in Figure 7 and Figure 8 respectively. The improvement in the acquisition time is more profound with the second order compared with the first order topology. This is due to the fact that the loop filter of the second order loop is triggered by double the loop DCO free running frequency. This will improve the climbing mechanism of the accumulation filter to reach the steady state in half the time required by the TDTL.
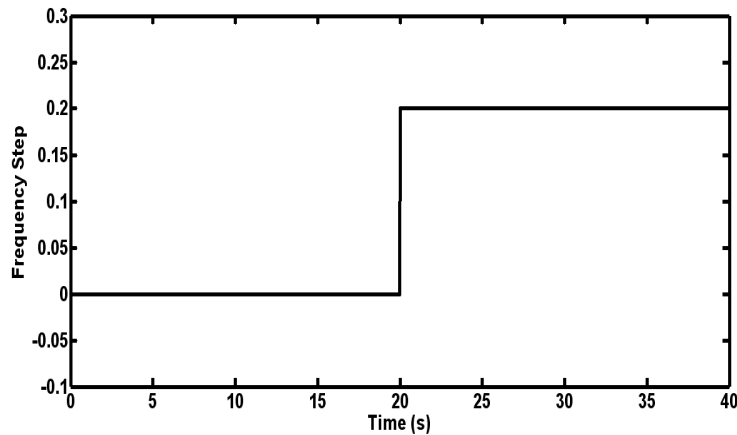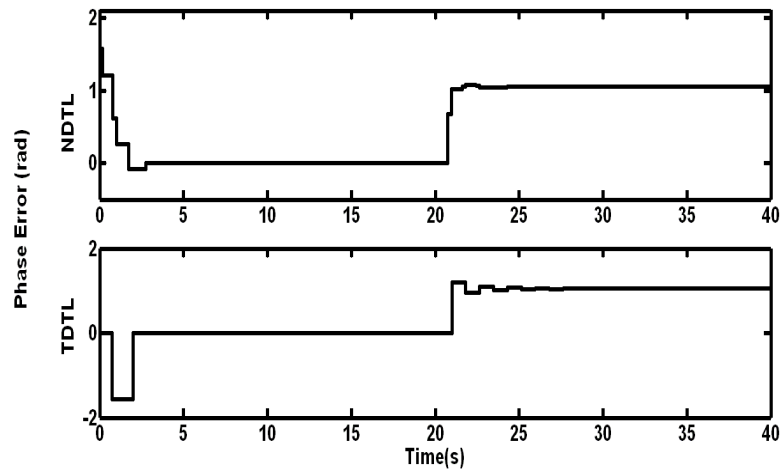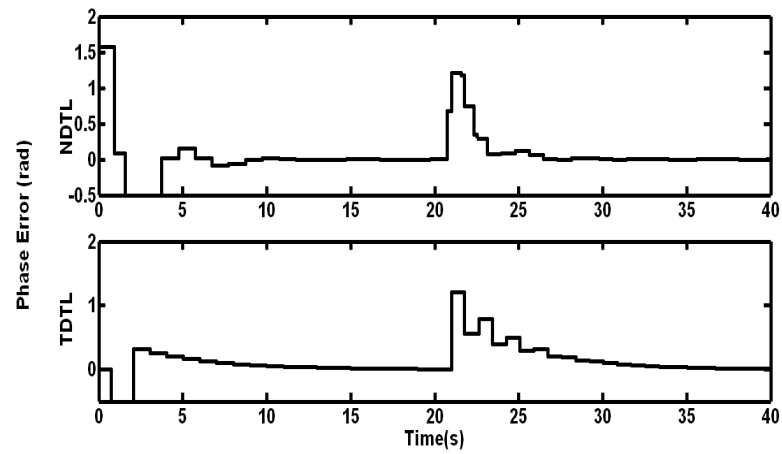

Figure 6 (a)

Figure 6 (b)

Figure 6 (c)

Figure 6. (a) Positive frequency step input (b) First-order NDTL and TDTL phase error responses and (c) Second-order NDTL and TDTL phase error responses with a positive frequency step of 0.2.
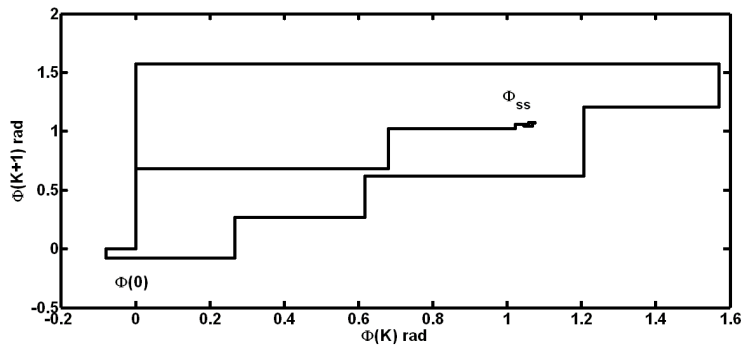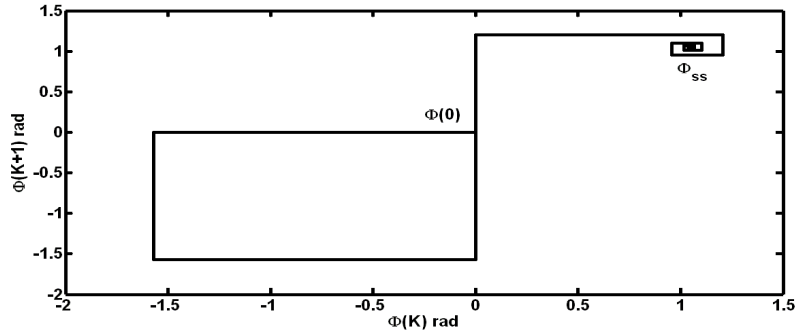

Figure 7(a)

Figure 7(b)

Figure 7. First-order phase planes of (a) NDTL (b) TDTL with a positive frequency step of 0.2.
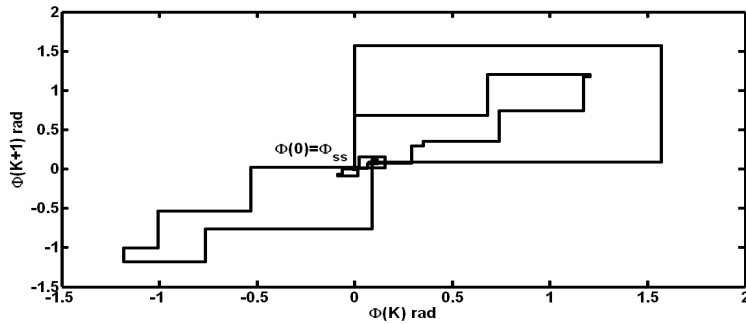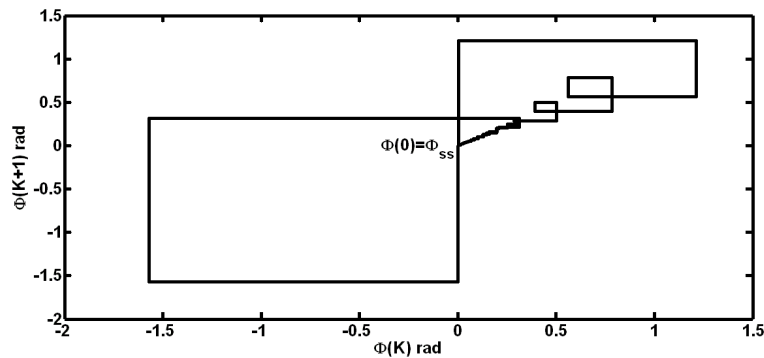

Figure 8(a)

Figure 8(b)

Figure 8. Second order phase planes of (a) NDTL (b) TDTL with a positive frequency step of 0.2.

The NDTL system was also tested with FSK input signal in noise-free environment and the results, for FSK demodulation, are shown in Figure 9. It is clear that the acquisition time of the NDTL is three times faster that of the TDTL. This is

attributed to the fact that the NDTL uses a DCO with double free running frequency, i.e. shorter intervals between the zero crossing, which reduces both the phase error and acquisition time.
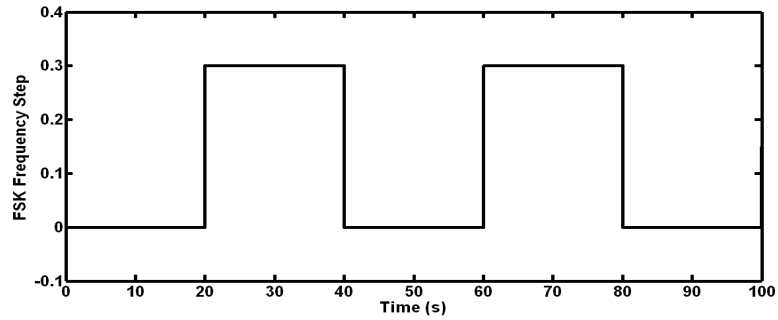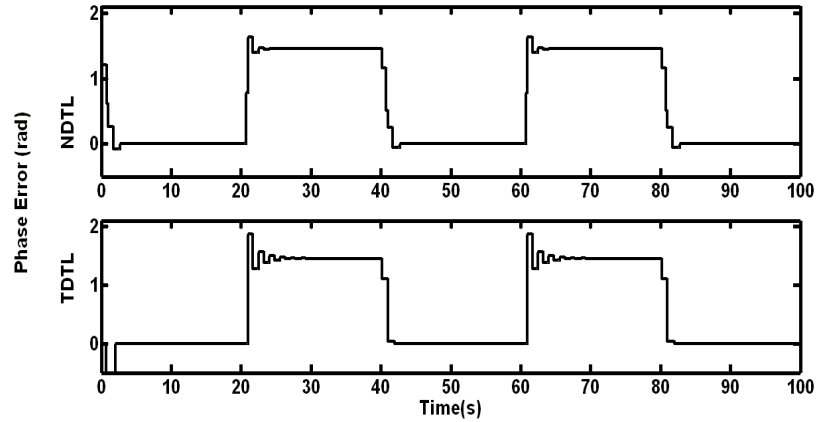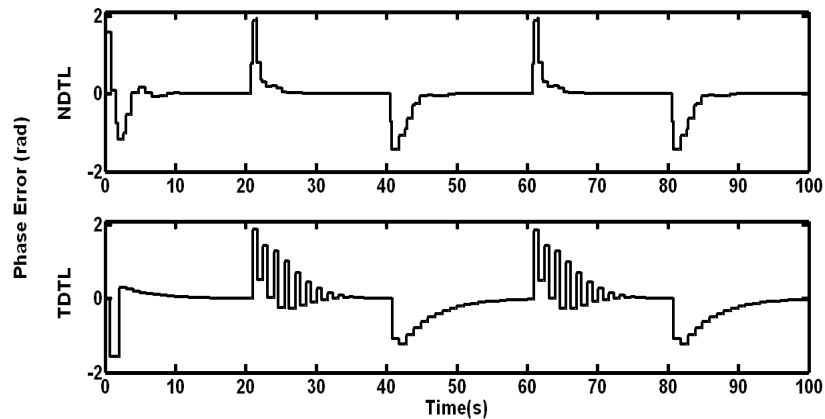

Figure 9(a)

Figure 9(b)

Figure 9(c)

Figure9. (a) FSK input (b) First-order NDTL and TDTL phase error responses and (c) Second order NDTL and TDTL phase error responses.

Another performance test was carried out under AWGN where both the first- and second-order NDTL were evaluated and compared with TDTL of the same order. Figure 10 shows the phase noise pdf for the first-order NDTL and TDTL for input SNR=7 dB. The figure shows the pdf for various input frequency steps. It is clear, from Figure 10 that the first-order NDTL has better performance than the TDTL when positive or negative frequency steps were applied. Furthermore, it is evident from Figure 10, that the NDTL margin of performance improvement increases with the increase in the input frequency step. This results from the additional phase error that the time delay block in the TDTL brings to the system as the input signal frequency increases. Figure 11 shows the phase noise pdf for the second order NDTL and TDTL systems for an input of SNR=7 dB when applying various step inputs. It is clear that the NDTL system outperformed the TDTL especially for higher frequency steps.

The final test is jitter performance, which is evaluated by comparing the difference in time of the zero crossing point between the original signal in noise-free environment and the NDTL output affected by the AWGN noise. Jitter values have a critical impact on many communication systems. The impact of noise on the jitter performance was tested and the results are illustrated in Figure 12 which indicates that the NDTL outperforms the TDTL as the SNR ratio decreases. For the second-order loop, the NDTL is slightly better than the TDTL.
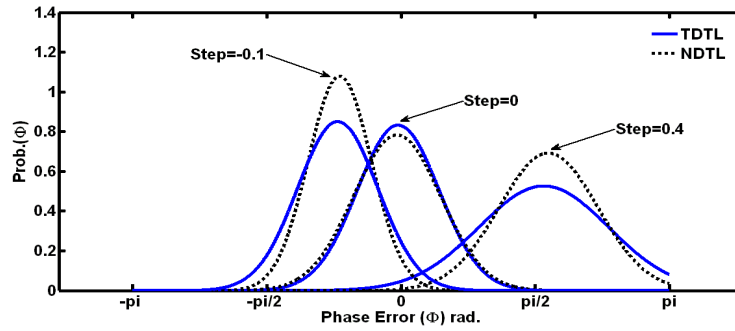
Figure 10. Steady-state pdf of phase error of first-order system for different frequency steps and SNR=7dB.
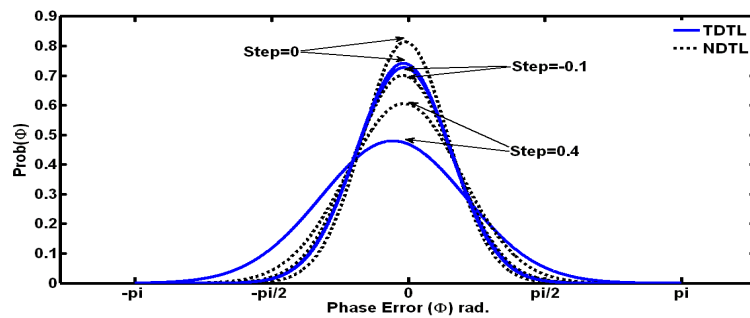

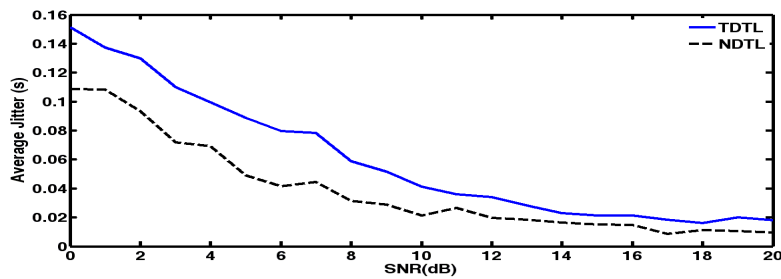Figure 11. Steady-state pdf of phase error of second-order system for different frequency steps and SNR=7dB.
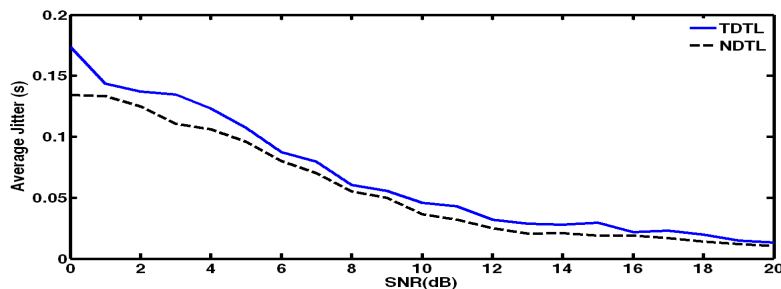

Figure 12 (a)

Figure 12 (b)

Figure 12. Jitter performance for a range of SNR (a) First order (b) Second order , frequency step of 0.1, and $K_1 = 1$.

5.   TDTL and NDTL Implementation

The viability of implementing the TDTL on a reconfigurable platform that uses an FPGA (field programmable gate array) was investigated in previous work [13,21]. It was demonstrated that the real time performance of the TDTL closely resembles the simulation results achieved using the model developed for MATLAB/Simulink.   The synthesis process of the prototype TDTL used a Xilinx System Generator to generate the necessary HDL (hardware description language) for the device-optimized block-set from within Simulink.   The structure of the reconfigurable first-order TDTL is shown in Figure 13 [13].
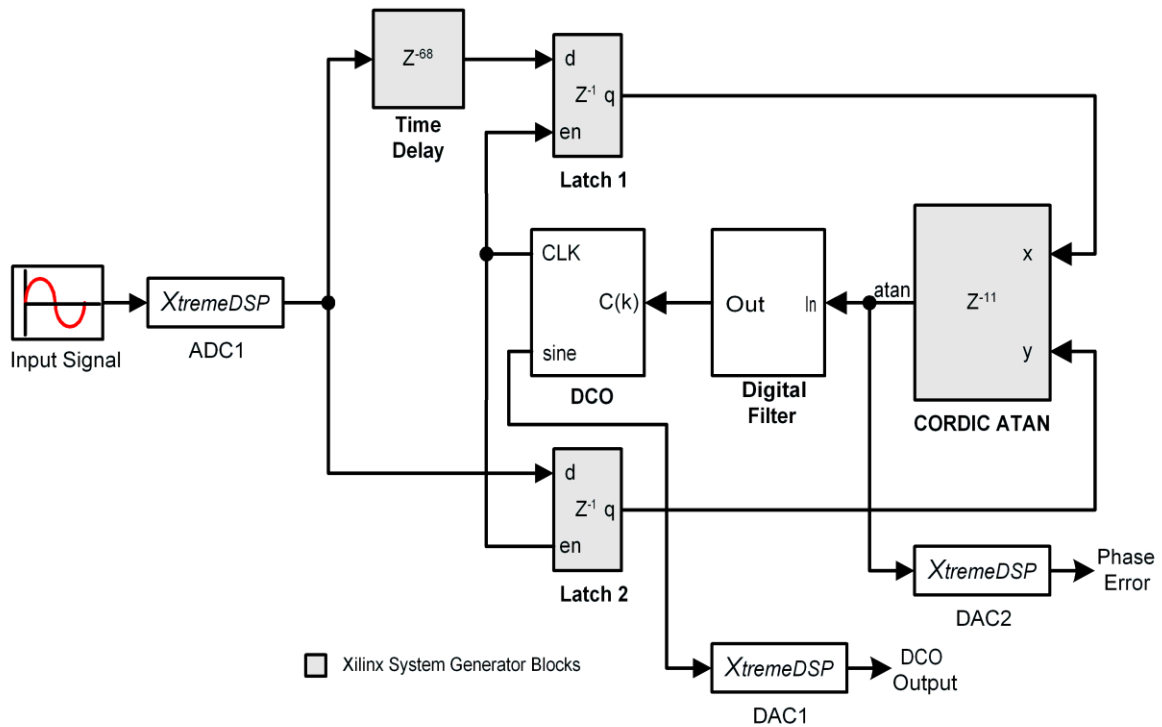

Figure 13. Structure of the reconfigurable TDTL

In the FPGA implementation depicted in Figure 13, the system block that is relatively complex to implement is the arctan phase detector.   This was implemented

using the CORDIC algorithm, which can translate trigonometric functions into the necessary digital circuits [22]. Overall the TDTL used a small part of the FPGA chip.

The focus of the research work in this paper is on the system architecture. The validity of the simulation model of the original TDTL was verified through comparison with physical implementation in the earlier work outlined above. Having said that, comparing the NDTL and the TDTL it is possible to see that the modified DCO only requires two additional flip-flops which is a very small cost in terms of gate count. At the same time, the NDTL does not require the delay block which may need to be a true analogue block in some applications. Optimized implementation of the NDTL, as well as other TDTL architectures, in a practical system will depend on the overall system specifications and the target technology. For example, synthesis for full-custom or ASIC (application specific integrated circuit) implementation can result in more optimized circuitry compared with that for an FPGA.

6. Conclusion

A digital tanlock loop with no time delay unit (NDTL) has been proposed. The system uses two sampling frequencies with a phase shift of $\pi/2$ (rad) to preserve the quadrature sampling relationship between the two loop channels. This enhances the linearity of the phase detector characteristics of the TDTL. The system was evaluated in the presence as well as in the absence of noise. The acquisition performance was assessed, in a noise-free environment, by subjecting it to frequency steps that cause sudden changes in the DCO free running frequency. In addition, the acquisition performance was also evaluated using FSK input signal. The NDTL system performance showed a clear improvement in the acquisition time compared with the TDTL. The improvements in the results are even more

pronounced with the second-order NDTL. The acquisition is shown to be three times faster with the new loop compared to the TDTL system.

By adding AWGN to the input signal, two performance evaluation tests were performed. They included the pdf and phase noise (jitter). Both tests indicated that the NDTL system outperformed the TDTL. For the pdf test, the first-order NDTL has better performance than the TDTL when positive or negative frequency steps were applied. The margin of improvement increases with the increase of the input frequency step. This results in additional phase error (i.e. non-linearity) that the time delay block in the TDTL brings to the system as the input signal frequency increases. For the second-order systems, the NDTL system outperformed the TDTL especially for higher frequency steps. The impact of noise on the jitter performance shows that both first- and second- order NDTL systems have better jitter compared with TDTL. Further, the proposed NDTL system can be entirely digitally implemented which reduces circuit complexity.

References

[1]Gardner, F.M., (2005), *Phase lock Techniques*, 3rd Edition, New York, USA: John Wiley.
[2]Best, R.E. (2007), *Phase-Locked Loops: Design, Simulation, and Applications*, New York: McGraw-Hill.
[3]Guan-Chyun H. and Hung,J. C. (1996), Phase-locked loop techniques. A survey, *IEEE Transactions on Industrial Electronics*, 43, 609-615.
[4]Stephens, D.R. (2001), *Phase-Locked Loops for Wireless Communications: Digital, Analog and Optical Implementations*, 2nd Edition, New York: Kluwer Academic Publisher.
[5]Crawford, J.A. (2007), Advanced Phase-Lock Techniques, USA: Artech House.
[6]Fitz, M.P., and Cramer, R.J. (April 1995), A Performance Analysis of a Digital PLL Based MPSK Demodulator, *IEEE Transactions on Communications*, 43, 1192-1201.
[7]Staszewski, R.B. et al, (Dec. 2005), 'All-digital PLL and transmitter for mobile phones', *IEEE J. Solid-State Circuits*, 40, 2469-2482.
[8]Kratyuk, V., Hanumolu, P.K., Moon, Un-Ku., and Maryaram, K. (March 2007), A Design Procedure for All-Digtal Phase-Locked Loops Based on a Charge-Pump

Phase-Locked-Loop Analogy, *IEEE Transactions on Circuits and Systems-II: Express Briefs*, Vol. 54, No.3, 247-251.

[9]McCune, E., (2010), *Practical Digital Wireless Signals*, UK: Cambridge University Press.

[10]Hussain, Z. M., Boashash, B. M., Hassan-Ali, and Al-Araji, S. R. (2001), A time-delay digital tanlock loop, *IEEE Transactions on Signal Processing*, 49, 1808-1815.

[11] Jae, L., and Chong, U. (1982), Performance Analysis of Digital Tanlock Loop, IEEE Transactions on Communications, vol. 30, pp. 2398-2411.

[12]Al-Araji, S. R., Hussain, Z. M., and Al-Qutayri, M. A. (2006), *Digital Phase Lock Loops: Architectures and Applications*, Dordrecht, the Netherlands: Springer.

[13]Al-Qutayri, M. A., Al-Araji, S. R., and N. I. Al-Moosa, (2006),'Improved First-Order Time-Delay Tanlock Loop Architectures', *IEEE Transactions on Circuits and Systems I: Regular Papers*, 53, 1896-1908.

[14]Al-Qutayri, M. A., Al-Araji, S. R., Al-Ali, O.A and Anani, N.A., (2009),Time delay digital tanlock loop with linearized phase detector, in the *proceedings of the 16th IEEE International Conference on Electronics, Circuits, and Systems, ICECS 2009*, IEEE, 555-558.

[15] Al-Araji, S.R., Al-Ali, Al-Araji, O.A., Al-Qutayri M.A., Anani, N.A and Ponnapalli, P.V. (2010), Improved performance second-order time-delay digital tanlock loop, in proceedings of the *33rd IEEE Sarnoff Symposium*, NJ, USA: IEEE, 1-5.

[16]Al-Ali, O. A., Al-Araji, S.R, Anani, N.A, Al-Qutayri, M.A and Ponnapalli, P.V. (May 2010), Adaptive TDTL using Frequency and Phase Processing Techniques, in the *proceedings of the IEEE Int. Conf. on Information Science, Signal Processing and their Applications (ISSPA 2010),* Malaysia: IEEE, 530-533.

[17]Haykin, S. (2008), *Communication Systems*, 4th Edition, New York: John Wiley & Son, Inc.

[18]Peebles Jr., P.Z. (2000), *Probability, Random Variables, and Random Signal Principles*, New York: McGraw-Hill.

[19]Kandeepan, S. (2009), 'Steady state distribution of a hyperbolic digital tanlock loop with extended pull-in range for frequency synchronization in High Doppler environment', *IEEE Transactions on Wireless Communications*, 8, 890-897.

[20]Mehrotra, A. (2002), 'Noise analysis of phase-locked loops', *IEEE Trans on Circuits and Systems-I: Fundamental Theory and Applications*, Vol. 49, No. 9, 1309-1316.

[21]Al-Araji, S., Al-Qutayri, M. and Al-Humaidan, A. (2008), 'Indirect Frequency Synthesizer using Second Order Digital Time Delay Tanlock Loop', *14th IEEE MELECON (2008)*, France.

[22]Gutierrez, R. and Valls, J. (2009), 'Low-Power FPGA-Implementation of *atan*(*Y/X*) Using Look-Up Table Methods for Communication Applications', *Journal of Signal Processing Systems*, Vol. 56, No. 1, 25-33.